

# SOLVING HYPERBOLIC PARTIAL DIFFERENTIAL EQUATIONS IN SPHERICAL GEOMETRY WITH RADIAL BASIS FUNCTIONS

NATASHA FLYER

## 1. INTRODUCTION

Mathematical modeling of space and climate phenomena generally requires the solution of partial differential equations (PDEs) inside/outside or on a sphere. A key difficulty is that it is impossible to uniformly distribute more than 20 points on a sphere, in contrast to trivially placing any number of points uniformly along the periphery of a circle. The essence of the problem is one that has faced cartographers for at least a millennium - the surface of a sphere cannot be mapped to a rectangle without severe distortions and a singularity in at least one location. Similarly, today's computational mathematicians are constantly grappling with the issue of how to devise efficient numerical methodologies for spherical domains, especially given the advent in the last decade of multi-processor distributed memory computers that are needed for large-scale simulations.

Currently used numerical methodologies all have specialized strengths but also serious weaknesses, mostly due to their association with an underlying grid. Global methods, such as double Fourier series or spherical harmonics, do not practically allow for local mesh refinement. The latter also involves cumbersome algebra, and can not be efficiently parallelized on multiprocessor machines. Localized methods, such as spectral element methods, have to refine near unphysical interior boundaries (due to element discretization as well as mapping onto a cube) in order to suppress Runge phenomena (violent oscillations near edges typical of high-order polynomial interpolation) and involve high algorithmic complexity. As a result, computational scientists in the field of climate and space modeling are scrambling for new options.

Radial basis functions(RBFs) offers a completely new numerical approach to the scientific community for solving time-dependent PDEs in spherical domains. This new methodology has the beauty of being grid-independent, allowing for non-uniform resolution, while providing spectrally accurate solutions to PDEs in multi-dimensions. However, the field is still in its development stage. The application of RBFs to pure hyperbolic systems has never been successfully addressed while the simpler problems of solving linear elliptic or parabolic PDEs in spherical geometries having only been addressed in the last three years. The few articles in the field are mainly of a theoretical nature, containing little or no computations or applications to physical modeling.

In the current presentation, we will give a brief overview of commonly used high-order methods for modeling spherical geometries, placing RBFs in this context. Next, we will derive the RBF formulation of the gradient operator in spherical coordinates that will be needed for solving the linear advection equation on a sphere. A method of lines formulation will be developed, illustrating how the discrete spatial differential operator is free of any singularities at the pole that are present in the original PDE when posed in spherical coordinates (and also present in other pseudospectral methods such as spherical harmonics). Secondly, the spectral accuracy of infinitely smooth RBFs will be demonstrated, showing high spatial accuracy for much lower resolution as compared to other spectral methods. In the oral presentation, time stability will be further analyzed along with other test cases.

---

*Key words and phrases.* Radial basis functions, hyperbolic PDEs, spheres .

## 2. OVERVIEW OF PRESENT HIGH-ORDER SPATIAL DISCRETIZATION METHODS FOR SPHERES

Below we discuss the three dominant classes of spectral methodologies that are currently used in climate and solar modeling (1, 2, 3). In part 4, we discuss the current state of RBFs in spherical geometries.

- (1) Double Fourier series method:

Standard spherical coordinates link  $\rho, \phi, \theta$  to the Cartesian coordinates  $x, y, z$  by

$$\begin{aligned}x &= \cos \phi \cos \theta, \\y &= \sin \phi \cos \theta, \\z &= \sin \theta.\end{aligned}$$

The domain exterior to a unit sphere is given by  $\rho \geq 1, -\pi/2 \leq \theta \leq \pi/2, -\pi \leq \phi \leq \pi$ . It usually is feasible to truncate the infinite extent in the r-direction by means of suitable asymptotic boundary conditions. However, both governing equations and physical grids will be singular at  $\theta = \pm\pi/2$ . This 'pole problem' can sometimes be partly overcome, e.g. in the double Fourier series method [6], [7], [1], [2] which takes note of the fact that all data is periodic in both the  $\phi$ -direction and  $\theta$ -direction. This permits the use of FFTs in both the angular directions, offering an attractive alternative to spherical harmonics, which are described next. However, it shares with these an inability to be combined with local mesh refinement.

- (2) Spherical harmonics:

For interpolation of functions defined on the periphery of a circle, Fourier expansions provide approximations with equal resolution everywhere. Expansions in spherical harmonics achieve the same feature over the surface of a sphere. However, there is no counterpart to FFTs for spherical harmonics. As a result, implementation of spherical harmonics in climate models require spectral transforms that are very costly.

- (3) Spectral elements on a cubed sphere:

Figure 1 illustrates a concept that has been used in some recent atmospheric models. As with the other methods mentioned in this overview, the inclusion of a radial direction is also relatively straightforward. The approach allows a limited amount of local mesh refinement and has been preferred in some recent atmosphere models [12], [13]. However, it requires high refinement near element boundaries to suppress the wild oscillations (Runge phenomenon) that occur for high order polynomial approximation needed to achieve spectral accuracy.

- (4) 'Classical' RBFs on sphere:

The concept of RBFs will be described in the next section. However, let us already note here that in the form RBFs are found in the present literature [4], [5], [8], [10] they allow for local mesh refinement only when implemented to low algebraic accuracy. Furthermore, these studies have been of a theoretical nature, primarily concerned with proving error bounds and convergence rates with applications only to solving the simple Poisson or heat equation in spherical geometry [3], [9].

Our approach that follows will be spectrally accurate for RBFs in spherical geometries, yet allows for local mesh refinement while providing stable time-stepping for purely advective equations.

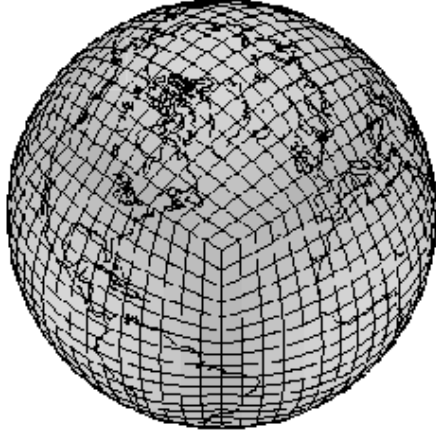


FIGURE 1. Illustration of mapping a sphere to spectral elements on a cube.

### 3. RBF FORMULATION OF GRADIENT OPERATOR

The radial function centered at the point  $\underline{x}_c$  is given by  $\psi(r^2 = \|\underline{x} - \underline{x}_c\|_2^2)$ , Next, let us define

$$q \equiv \|\underline{x} - \underline{x}_c\|_2^2.$$

The reason for doing so is that analytic derivatives are taken with respect to  $q$  as will be seen below. It is important to note that the distances are not great circle arcs measured along the surface but are the squared Euclidean norm measured straight through the sphere.

Now we restrict  $\underline{x}$  and  $\underline{x}_c$  to lie on the surface of the unit sphere, and change to longitude-latitude-type spherical coordinates, i.e.

$$(1) \quad \begin{aligned} x &= \cos \phi \cos \theta, \\ y &= \sin \phi \cos \theta, \\ z &= \sin \theta. \end{aligned}$$

(Note that this differs from traditional spherical coordinates in that we measure  $\theta$  from the equator rather than from the north pole). Then,

$$q = 2 - \cos \theta \cos \theta_c \cos(\varphi - \varphi_c) + \sin \theta \sin \theta_c,$$

and the partial derivatives of  $\psi$  with respect to  $\varphi$  and  $\theta$  are given by

$$(2) \quad \frac{\partial}{\partial \varphi} \psi(q) = 2 \cos \theta \cos \theta_c \sin(\varphi - \varphi_c) \frac{d\psi}{dq},$$

$$(3) \quad \frac{\partial}{\partial \theta} \psi(q) = 2(\cos \theta_c \cos(\varphi - \varphi_c) \sin \theta - \cos \theta \sin \theta_c) \frac{d\psi}{dq}$$

In our spherical coordinates, the gradient on the surface of the unit sphere is given by

$$\nabla = \frac{1}{\cos \theta} \frac{\partial}{\partial \varphi} \hat{\varphi} + \frac{\partial}{\partial \theta} \hat{\theta},$$

Clearly, the gradient has a singularity in the  $\varphi$  direction at the poles unless the derivative (with respect to  $\varphi$ ) of the underlying function also vanishes at the poles. We see from (2) that this is exactly what happens when using a radial function. Using (2) and (3), we have the action of the

gradient operator on the RBF scalar function

$$(4) \quad \nabla\psi(q) = 2 [\cos\theta_c \sin(\varphi - \varphi_c)\mathbf{i} + (\cos\theta_c \cos(\varphi - \varphi_c) \sin\theta - \cos\theta \sin\theta_c)\mathbf{j}] \frac{d\psi}{dq}$$

#### 4. A NUMERICAL TEST EXAMPLE: SOLID BODY ROTATION

The first test case, using the setup given in [14], simulates the advection of a height field  $h(\varphi, \theta)$  over the sphere at a direction forming an angle  $\alpha$  relative to the computational longitude ( $\varphi$ ) - latitude ( $\theta$ ) grid. The PDE to be solved is the advection equation in spherical coordinates given by

$$(5) \quad \frac{\partial h}{\partial t} + \frac{u}{a \cos\theta} \frac{\partial h}{\partial \varphi} + \frac{v}{a} \frac{\partial h}{\partial \theta} = 0$$

with the advecting wind being

$$(6) \quad u = u_0(\cos\theta \cos\alpha + \sin\theta \cos\varphi \sin\alpha)$$

$$(7) \quad v = -u_0 \sin\varphi \sin\alpha.$$

We will consider two initial conditions (which is also the solution for all time): 1) a cosine bell profile that is  $C^1$  and 2) an exceptionally steep Gaussian profile that is  $C^\infty$ . The initial cosine bell profile, Figure 3(a), that is to be advected without distortion by the above steady wind (6-7) is

$$h(\varphi, \theta) = \begin{cases} \frac{h_0}{2} (1 + \cos(\pi \frac{r}{R})) & r < R \\ 0 & r \geq R \end{cases}$$

where  $a$  is the radius of the earth,  $6.37122 \times 10^6$  m,  $h_0 = 1000$  m,  $u_0 = 2\pi a / (12 \text{ days} = 288 \text{ hours})$ ,  $R = a/3$  and  $r = a \arccos(\sin\theta_c \sin\theta + \cos\theta_c \cos\theta \cos(\varphi - \varphi_c))$ . The center of the bell is initially taken to be at the equator,  $(\varphi_c, \theta_c) = (3\pi/2, 0)$ . The Gaussian bell profile is similar (see Figure 3(b)).

Evaluating the spatial operator in (5) at the RBF nodes using the RBF formulation of the partial derivatives defined in the previous section leads to the discrete matrix operator

$$(8) \quad B_{i,j} = 2 \{ \cos\alpha \cos\theta_i \cos\theta_j \sin(\varphi_i - \varphi_j) + \sin\alpha [\cos\theta_i \cos\varphi_i \sin\theta_j - \cos\theta_j \cos\varphi_j \sin\theta_i] \} \frac{d\psi}{dq}$$

However, in order to solve the linear advection equation, we need the discrete differentiation matrix  $D$  that will act on our dependent variable  $h$  at each time step, i.e.  $DA = B$ , where  $A$  is the standard RBF interpolation matrix for the data (c.f. Bengt Fornberg's abstract),

$$(9) \quad A_{i,j} = \psi(\|\underline{x}_i - \underline{x}_j\|^2).$$

Then,  $D = BA^{-1}$  and a method of lines approach can be implemented.

$$(10) \quad \frac{\partial h}{\partial t} = Dh$$

Since  $B$  is antisymmetric, we can guarantee that  $D$  has a pure imaginary spectrum if  $A$  is positive definite [11] (as shown in Figure 2). Such a spectrum permits time steps that are much larger than allowed by other spectral methods. In the current study a classic fourth-order Runge-Kutta method is used.

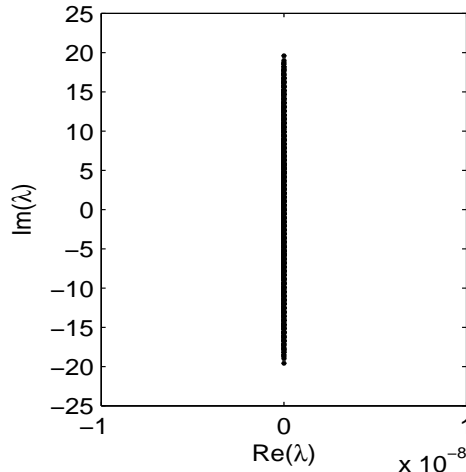


FIGURE 2. Eigenvalue spectrum of the RBF differentiation matrix  $D$

## 5. RESULTS

Figures 3(a) and 3(b) show the initial profiles that are advected, followed directly below in Figures 3(c) and 3(d) by the error norms on a log-log and log-linear plot, respectively. As can easily be seen, the RBF method for the cosine bell profile converges quadratically due to a jump in the second derivative while the Gaussian bell exponentially converges since the initial condition is infinitely smooth. In the oral presentation, we look more in depth into the eigenvalue stability analysis of the differentiation matrix  $D$  and consider other test cases that illustrate the power and beauty of the RBF methodology for hyperbolic PDEs.

## REFERENCES

- [1] Fornberg, B., *A Practical Guide to Pseudospectral Methods*, Cambridge University Press, 1996.
- [2] Fornberg, B. and Merrill, D., Comparison of finite difference- and pseudospectral methods for convective flows over a sphere, *Geophys. Res. Lett.* 24 (24) (1997), 3245-3248.
- [3] Gia, Q.T., Approximation of parabolic PDEs on spheres using spherical basis functions, *Adv. Comput. Math.*, To appear.
- [4] Golitschek, M.v., and Light, W.A., Interpolation by polynomials and radial basis functions on spheres, *Constr. Approx.*, 17 (2001), 1-18.
- [5] S. HUBBERT AND T. MORTON,  $L^p$ -error estimates for radial basis function interpolation on the sphere, *J. Approx. Theory*, 129 (2004), pp. 58-77.
- [6] Merilees, P.E., The pseudospectral approximation applied to the shallow water equations on a sphere, *Atmosphere*, 11 (1), (1973), 13-20.
- [7] Merilees, P.E., Numerical experiments with the pseudospectral approximation in spherical coordinates, *Atmosphere*, 12 (3) (1974), 77-96.
- [8] Mhaskar, H.N., Narcowich, F.J. and Ward, J.D., *Representing and Analyzing Scattered Data on Spheres, Multivariate Approximation and Applications*, edited by N. Dyn, D. Leviatan, D. Levin, and A. Pinkus, Cambridge University Press, Cambridge, U. K., 2001.
- [9] Morton, T.M. and Neamtu, M., Error bounds for solving pseudodifferential equations on spheres by collocation with zonal kernels., *J. Approx. Theory*, 114(2), (2002), 242-268.
- [10] Narcowich, F.J., and Ward, J.D., *Scattered data interpolation on spheres: error estimates and locally supported basis functions*, *SIAM J. Math. Anal.*, 33(6), (2002), 1393-1410,.
- [11] R. B. PLATTE AND T. A. DRISCOLL, Eigenvalue stability of radial basis function discretizations for time-dependent problems, *Comput. Math. Appl.* To appear 2006.

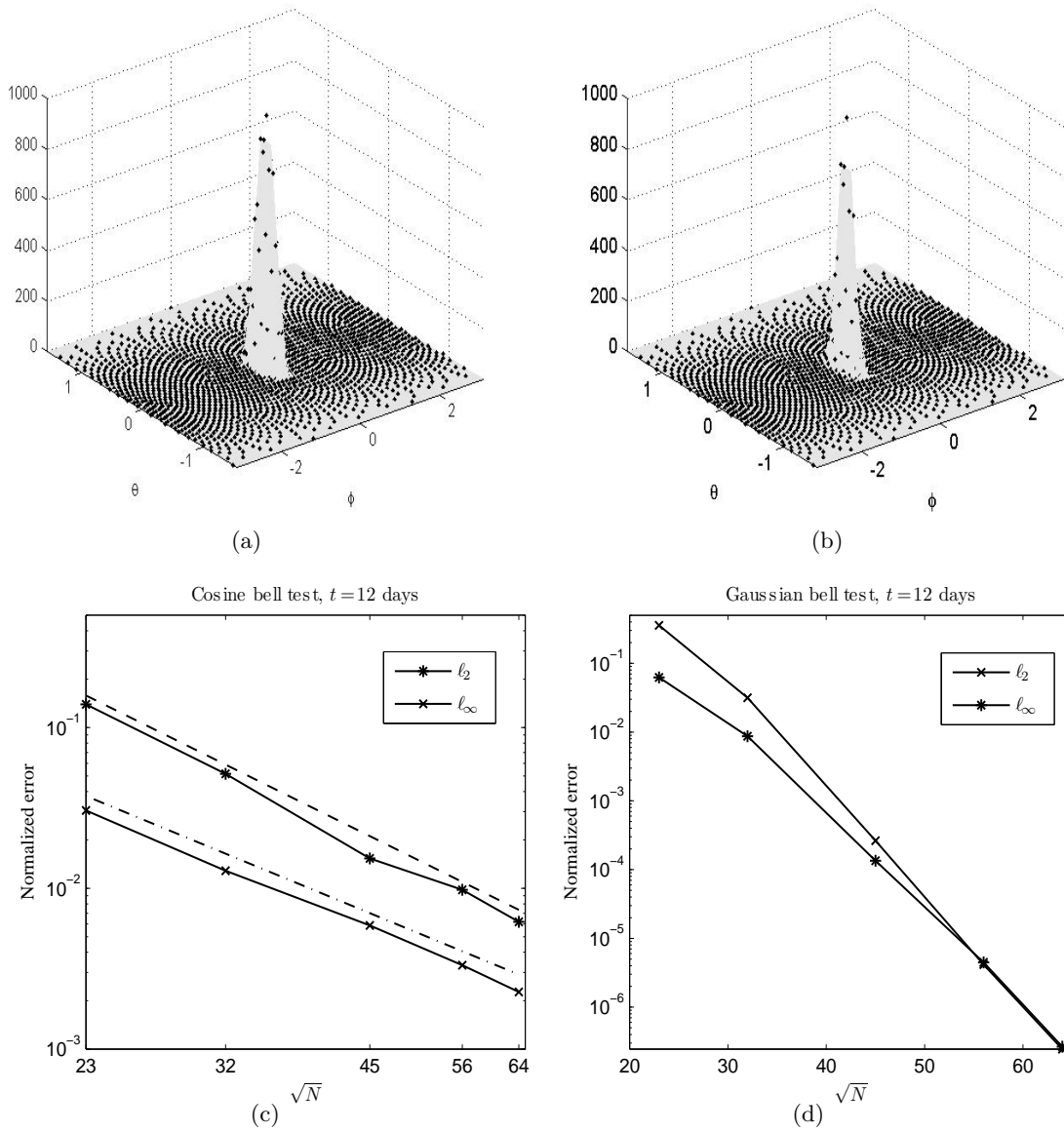


FIGURE 3. (a) Cosine bell initial condition on an 'unrolled' sphere (b) Gaussian bell initial condition (c)  $\ell_\infty$  and  $\ell_2$  error norms for the cosine bell profile as a function grid spacing  $h$  ( $h \sim 1/\sqrt{N}$ , where  $N$  is the number of nodes). The dashed lines plot  $ch^{-2}$ , for some constant  $c$ . (d)  $\ell_\infty$  and  $\ell_2$  error norms for the Gaussian bell profile

- [12] Rancic, M., Purser, R.J., Mesinger, F., A global shallow water model using an expanded spherical cube: Gnomonic versus conformal coordinates, *Q.J.R. Meteorol. Soc.*, 122 (1996), 959-982.
- [13] Taylor, M., Tribbia, J., Iskandarani, M., The spectral element method for the shallow water wave equations on the sphere, *J. Comp. Phys.*, 130 (1997), 92-108.
- [14] D. L. WILLIAMSON, J. B. DRAKE, J. J. HACK, R. JAKOB, AND P. N. SWARZTRAUBER, A standard test set for numerical approximations to the shallow water equations in spherical geometry, *J. Comput. Phys.*, 102 (1992), pp. 211-224.